View metadata, citation and similar papers at core.ac.uk

brought to you by CORE

provided by Elsevier - Publisher Connector

Procedia Manufacturing

Volume 5, 2016, Pages 478–494

44th Proceedings of the North American Manufacturing Research Institution of SME http://www.sme.org/namrc

Improved Process Geometry Model with Cutter Runout and Elastic Recovery in Micro-End Milling

Tesfaye M. Moges[1], K.A. Desai[2,*] and P.V.M. Rao[1]

[1]*Indian Institute of Technology Delhi, New Delhi, India.*

[2]*Indian Institute of Technology Jodhpur, Jodhpur, India.*

tesfaye_mom@yahoo.com, kadesai@iitj.ac.in, pvmrao@mech.iitd.ac.in

Abstract

A process geometry model determines engagement angle and instantaneous uncut chip thickness which forms basis in predicting cutting forces and surface quality in micro-end milling operation. This paper presents a process geometry model incorporating cutter runout, elastic recovery of work material and minimum chip thickness. These characteristics are incorporated effectively by realizing different engagement cases that are likely to occur during micro-milling. The model considers interactions of tooth trajectory under consideration with surfaces generated by previous teeth to develop a realistic process geometry model. It has been demonstrated that the inclusion of tooth trajectory interactions has significant effect on prediction accuracy of a model. The results are also substantiated by conducting machining experiments at various cutting conditions.

Keywords: Micro-end milling, engagement angle, chip thickness, tooth trajectory interactions, cutter runout, elastic recovery

1 Introduction

The application of complex miniaturized components is increasing considerably in automobile, medical and electronics industries. Micro-milling is preferred over other processes to produce micro-components as it is capable of processing a wide range of materials with higher accuracy and at lower cost (Chae et al, 2006). Micro-milling is a down-scaled version of conventional milling and thus both processes are similar from operational point of view but significant differences exist in cutting phenomena and mechanics of chip formation (Cheng and Huo, 2013). The process uses multi-tooth cutter and removes work material due to rotary and translating motions between cutting tool and workpiece. Martellotti (1941) showed that the path of milling tooth is trochoidal and presented parametric expressions for a tooth trajectory. Many researchers approximated the trajectory of cutting teeth as circular while determining process geometry, cutting forces and surface error for conventional

* Corresponding author

 Selection and peer-review under responsibility of the Scientific Programme Committee of NAMRI/SME
© The Authors. Published by Elsevier B.V.

doi:10.1016/j.promfg.2016.08.040

milling (Martellotti, 1945, Tlusty and Macneil, 1975) and micro-milling operations (Kim et al, 2004). Bao and Tansel (2000a) showed that the circular trajectory approximation for a cutting tooth results into significant error while predicting process geometry for micro-milling. This is primarily due to larger ratio of feed per tooth to tool radius compared to conventional milling which necessitates considering trochoidal tooth trajectory.

Another important aspects of micro-milling process is elastic recovery of work material at low chip thickness values. The edge radius of micro-end mill is comparable in size with uncut chip thickness (Wuele et al, 2001). When chip thickness is less than certain minimum value, material removal does not occur in micro-milling. The ploughed material flows under the edge of a tool and material gets elastically recovered which rubs the flank face (Vogler et al, 2004, Park and Malekian, 2009). The subsequent cutting edge removes elastically recovered material withstanding higher chip load.

As micro-milling operation involves use of a multi-tooth cutter rotating about an axis, cutter runout is another issue which is expressed as deviation of cutting tooth from its axis of rotation. In the presence of cutter runout, material removed by each cutting tooth is not identical with certain edges removing more material. The unequal distribution of chip load leads to varying cutting forces among teeth and poor surface quality. Bao and Tansel (2000b) studied the variation of cutting tooth trajectories at different cutter runout parameters and showed that the effect of runout is noticeable in micro-milling. Jun et al. (2006) developed a chip thickness model considering elastically recovered, mixed elastic-plastic and complete material removal of regions in micro-milling process. The effect of elastic recovery on cutting forces was studied by Malekian et al. (2009) and Jun et al. (2012) considering similar chip thickness model. Afazov et al. (2010) analyzed the effect of cutter runout on instantaneous uncut chip thickness and reported its significance at lower feed rate values. However, interaction between tooth trajectories was not considered in these studies which can lead to significantly different values of process geometry parameters. Uriarte et al. (2008) proposed cutting force model for ploughing and shearing dominant regions of cutting zone considering minimum chip thickness. Wu et al. (2012) investigated the effect of different tool geometries on process performance of micro-milling using Finite Element Method (FEM). It has been observed that the edge radius has significant effect on cutting forces. Malekian et al. (2012) formulated minimum chip thickness model using minimum energy principle and infinite shear strain method for rounded-edge tool. It has been observed that the minimum chip thickness depends on tool geometry and properties of workpiece material. Kang and Zheng (2013) developed a chip thickness model for micro-milling process using Fourier analysis but it does not incorporate cutter runout, minimum chip thickness and elastic recovery of workpiece material. Srinivasa and Shunmugam (2013) proposed a methodology to predict cutting force coefficients by considering the effects of edge radius and workpiece properties. The sweep angle caused by helical end mill is included in engagement angle computation which used for further in determining integration limits to calculate cutting forces. Jing et al. (2014) developed a methodology to incorporate the effect of cutting tool geometry and workpiece properties while determining uncut chip thickness. The study also examined the effect of cutting conditions such as feed rate, depth of cut and cutting speed on cutting forces. Recently, De Oliveira et al. (2015) proposed a methodology to determine minimum chip thickness experimentally by correlating it with specific cutting force and surface roughness. The study concluded that it varies between $1/4^{th}$ to $1/3^{rd}$ of the edge radius regardless of tool geometry and properties of workpiece material.

Various studies on micro-milling as discussed above highlighted the effect of process characteristics such as elastic recovery of work material, cutter runout, minimum chip thickness etc. It was assumed in these studies that the current tooth trajectory interacts only with immediately preceding tooth trajectory. However, in the presence of cutter runout and at relatively smaller values of feed rate which are quite common in micro-milling, it may not be effective. The current tooth trajectory may interact with more than one previous tooth trajectories and cause significant changes in the nature of engagement for a cutting edge. This paper presents determination of process geometry parameters by considering tooth trajectory interactions, cutter runout, elastic recovery of work material and minimum chip thickness.

The paper determines engagement angle and instantaneous uncut chip thickness with and without tooth trajectory interactions and validates the effectiveness of the proposed approach by comparing results with machining experiments.

The mathematical model determining engagement angle and uncut chip thickness considering tooth trajectory interactions in the presence of cutter runout and elastic recovery is given in Section 2. Section 3 presents computational results of the proposed model and the effect of tooth trajectory interactions and elastic recovery on process geometry parameters. The results of machining experiments are also discussed in this section to validate the effectiveness of the proposed model. The outcomes of the present work are summarized in Section 4.

2 Modelling Process Geometry in Micro-Milling

Modelling of process geometry in micro-milling requires determining engagement angle and instantaneous uncut chip thickness for each cutting edge. The methodology determines process geometry by dividing the operation into discrete steps; angle by angle, flute by flute and finally dividing the cutter into finite axial segments slice by slice (Altintas, 2000). As highlighted in the previous section, it is required to consider true tooth trajectory including rotational and translational motions between tool and workpiece to determine process geometry parameters accurately. The true trajectory of a cutting edge depends on tool radius, tool runout, feed rate and angular rotation of the tool. The parametric representation of true tooth trajectory in the presence of cutter runout can be expressed as Equation (1) (Bao and Tansel, 2000b).

$$\left.\begin{aligned} x(k,i) &= \frac{N_t * fpt}{2\pi}\theta + rsin(\varphi) + (-1)^i * \rho\sin(\varphi+\gamma) \\ y(k,i) &= rcos(\varphi) + (-1)^i * \rho\cos(\varphi+\gamma) \end{aligned}\right\} \quad (1)$$

Here, k and i are indices for axial disc elements and cutting edges respectively, N_t is number of teeth, fpt is feed per tooth, θ is cutter rotation angle for the bottom most point of a cutting edge from Y axis, r is cutter radius, ρ is cutter runout offset and γ is runout orientation angle. The cutting edge trajectories of a micro-end mill can be determined using equation (1). The instantaneous angular position (φ) of i^{th}cutting edge at an axial depth of cut value dz can be determined using Equation (2) (Altintas, 2000).

$$\varphi = \theta - i * \varphi_p - (k-0.5) * dz * \frac{\tan(\theta_{hx})}{\mathrm{r}} \quad (2)$$

Here, φ_p is pitch angle i.e. the angle between two consecutive teeth of a cutting tool, dz is the thickness of an axial disc element and θ_{hx} is helix angle of a cutter.

As the ratio of runout to cutter diameter is quite large in micro-milling, the effect of cutter runout is significant and it must be considered while computing process geometry parameters. It determines chip load experienced by each cutting edge and level of interaction between trajectories. At smaller values of feed rate, it is quite common that only one cutting edge removes entire material while the other cutting edge does not engage in the cut (Bao and Tansel, 2000b and Afazov et al. 2010). Another important aspect of micro-milling is the elastic recovery of work material at small feed rate. When chip thickness is less than certain minimum value, ploughed material flows under the edge of the tool and recovers elastically.

It has been observed that the tooth trajectory under consideration may interact with more than one preceding tooth trajectories in the presence of cutter runout for conventional end milling process (Desai, et al. 2009). This necessitates evaluation of a tooth trajectory with past teeth trajectories in determining process geometry. The distribution of chip load is uneven between cutting edges in the presence of tool runout. The cutting edge removing more material is termed as *'high'* tooth while the one removing less material is termed as *'low'* tooth. Based on level of interaction between trajectories, three cases are

formulated in the study to analyse the interaction of trajectories. These cases are general and discussed for a micro-end mill with two cutting teeth in the present study. The cases are illustrated in Figure 1(a) to (c).

Case-I: Both *'high'* and *'low'* trajectories interact with immediately preceding teeth trajectories respectively (Figure 1(a)). This occurs at higher feed rate and very small magnitude of cutter runout. This situation is common for milling operation where the ratio of runout to diameter is quite small.

Case-II: Both *'high'* and *'low'* tooth trajectories interact with the preceding *'high'* tooth trajectory only (Figure 1(b)). This primarily occurs at relatively lower value of feed rate and in the presence of runout.

Case-III: A *'high'* tooth trajectory interacts with preceding *'high'* tooth trajectory and no interaction of *'low'* tooth trajectory as it is not in contact with the workpiece (Figure 1(c)). This occurs at very small feed rate and higher values of cutter runout.

Based on these different cases of engagement, the methodology to determine process geometry parameters in the presence of cutter runout and elastic recovery is presented in subsequent sub-sections.

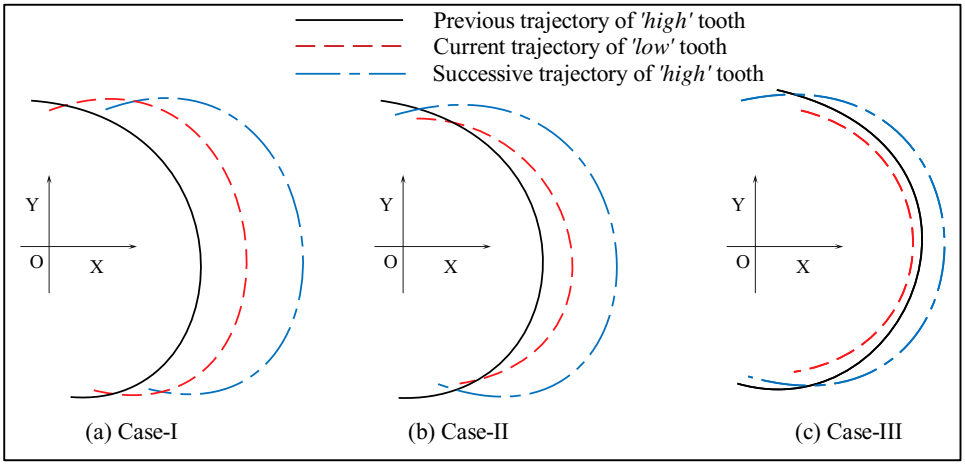

Figure 1. Interaction of cutting edge trajectories in the presence of cutter runout.

2.1 Determination of Engagement Angle

The engagement angle represents the duration for which a cutting teeth is engaged with the workpiece. Mathematically, it is expressed as the difference between an angle at which cutting teeth engages into the cut and an angle at which it exits from the cut. The cutting edge enters into or exits from the cut when current trajectory intersects with the surface generated by the preceding edge. The methodology proposed in this paper uses the coordinates of tooth entry and exit points along with coordinates of tool centre location to determine engagement angle.

Figure 2 depicts the procedure to compute coordinates of these points geometrically and thereby an engagement angle. Referring to Figure 2(a), P_1 and Q_1 are the entry and exit points of a cutting tooth under consideration based on its intersection with immediately previous trajectory (Case-I). Thus $P_1\hat{C}_1Q_1$ represent engagement angle of the current tooth. It has to be noted that C_1 is the centre of cutting tool corresponding to entry point P_1. The coordinates of P_1 and Q_1 are determined using Equation (1) while the final values are selected based on the minimum distance. As feed motion is along X-axis, the coordinates of centre point C_1 at a particular angular position of the tool in the presence of runout can be obtained from Equation (3).

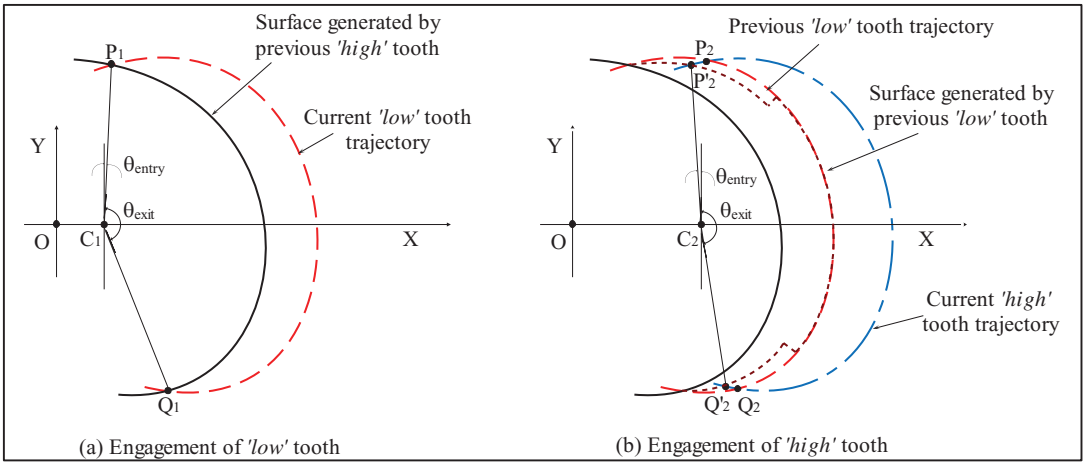

Figure 2. Representation of entry and exit angles of *'low'* and *'high'* tooth

$$\left.\begin{aligned} X_c &= \frac{N_t * fpt}{2\pi}\theta + (-1)^i * \rho \sin(\varphi + \gamma) \\ Y_c &= (-1)^i * \rho \cos(\varphi + \gamma) \end{aligned}\right\} \tag{3}$$

Considering trajectory of previous tooth as surface generated, the entry angle (θ_{entry}) of current tooth can be calculated using coordinates of $P_1(X_{P1}, Y_{P1})$ and $C_1(X_{C1}, Y_{C1})$ as Equation (4). Similarly, the exit angle of current tooth can be calculated using coordinates of $Q_1(X_{Q1}, Y_{Q1})$ and $C_1(X_{C1}, Y_{C1})$ as Equation (5).

$$\theta_{entry} = \tan^{-1}\left(\frac{X_{P1} - X_{C1}}{Y_{P1} - Y_{C1}}\right) \tag{4}$$

$$\theta_{exit} = \pi - \tan^{-1}\left(\frac{X_{Q1} - X_{C1}}{Y_{Q1} - Y_{C1}}\right) \tag{5}$$

The engagement angle, θ_{eng} is the difference between entry and exit angle and it can be computed using Equation (6).

$$\theta_{eng} = \theta_{exit} - \theta_{entry} \tag{6}$$

In order to determine engagement angle, centre location of the tooth under consideration and its intersection with surfaces generated by previous teeth are required. Equations (3)-(6) uses trajectory of a cutting tooth to determine engagement angle. But in micro-milling operation, surfaces generated by previous teeth are not same as its trajectories due to elastic recovery of work material (Jun et al. 2006 and Malekian et al. 2009). As the edge radius of cutting tool is large in micro-milling, material is not removed when instantaneous uncut chip thickness is less than the limiting value. In this case, it flows under the edge of the tool and certain portion of it is recovered elastically. The actual work surface generated due to elastic recovery is shown schematically using dotted curve in Figure 2(b). It can be seen that P_2 and Q_2 are entry and exit points when elastic recovery is not considered. Due to elastically recovered work material, current tooth trajectory intersects with the surface generated from previous tooth at point P'_2 and Q'_2. The modified coordinates of tooth entry and exit points can be determined considering height of elastically recovered work material. The amount of material recovering elastically can be expressed as certain percentage of chip thickness in elastic-plastic region (Jun et al., 2006). When chip thickness is less than the minimum value in ploughing dominant region, the height of elastically recovered material can be determined using Equation (7) which is expected to be removed by next tooth.

$$h_{er} = p_e h \quad (7)$$

As feed rate is quite small in micro-milling, Case-II and III are likely to occur frequently. For engagement Case-II, R_1 and R_2 are entry and exit points of a *'low'* tooth which can be determined using intersection of current trajectory with surface generated by immediately previous *'high'* tooth as shown in Figure 3. This results into $R_1\hat{C}_1R_2$ as the engagement angle of *'low'* tooth under consideration. Similarly for Case-III, entry and exit points of a *'high'* tooth are determined based on intersection of trajectory under consideration with surface generated by previous *'high'* tooth. In case-III, *'low'* tooth does not engage in the cut and its trajectory (as shown in Figure 3 using short dashed curve) does not interact with any surface.

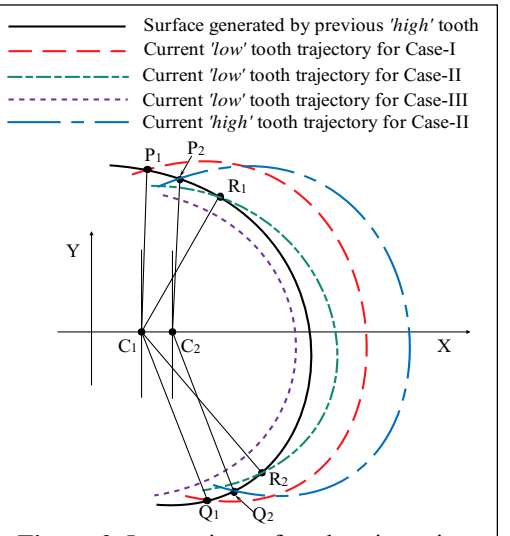

Figure 3. Interactions of teeth trajectories of *'low'* and *'high'* tooth for Case-I, II and III

2.2 Determination of Uncut Chip Thickness

Another important element of a process geometry model is instantaneous uncut chip thickness. The removal of material occurs in micro-milling when chip thickness is greater than the minimum value and the region in which chip forms is known as shearing dominant region. When chip thickness is less than the minimum limiting value, ploughing action is dominant instead of shearing and material removal does not occur which is termed as ploughing dominant region (Chae et al, 2006, Vogler et al, 2004 and Park rand Malekian, 2009). The cutting zone is divided into two regions for the purpose of computing chip thickness; shearing and ploughing dominant region. The instantaneous uncut chip thickness in shearing dominant region is expressed as the shortest radial distance between the cut surface and trajectory of the cutting edge at a given rotation angle. Considering successive tooth trajectories, instantaneous uncut chip thickness can be expressed as the radial distance between surfaces generated by these two trajectories as geometrically depicted in Figure 4(a).

At a given rotation angle (φ), instantaneous uncut chip thickness is depicted as distance $\overline{NM}$ which can be mathematically expressed using Equation (8). The coordinates of point $C\ (x_C, y_C)$ and $M\ (x_M, y_M)$ at a given tool rotation angle can be determined using Equations (3) and (1) respectively. The coordinates of point $N\ (x_N, y_N)$ are determined by computing the shortest distance between line $\overline{CM}$ and the coordinates of previously generated workpiece surface.

$$h = \overline{NM} = |\overline{CM} - \overline{CN}| \quad (8)$$

When uncut chip thickness h is less than the minimum value, ploughed material is not removed in form of a chip; instead it flows under the flank face of the tool and undergoes elastic-plastic deformation. Figure 4(b) shows ploughing and shearing dominant region along with the effect of elastic recovery in micro-milling. The workpiece surface generated considering elastic recovery in ploughing dominant region is shown using dotted curves in Figure 4(b). In this region, surfaces generated by teeth and its trajectories are not identical due to elastic recovery of work material. Therefore, point N which is located on previous tooth trajectory cannot be used in determining chip thickness. This necessitates determination of point N' located on the surface generated after elastic recovery. The modified surface generated due to elastic recovery of work material has been derived considering height of elastically recovered material. The coordinates of elastically recovered surface can be determined using Equation

(9). The coordinates of intersection point $N'(x_{N'}, y_{N'})$ are determined in the same manner as point N discussed earlier.

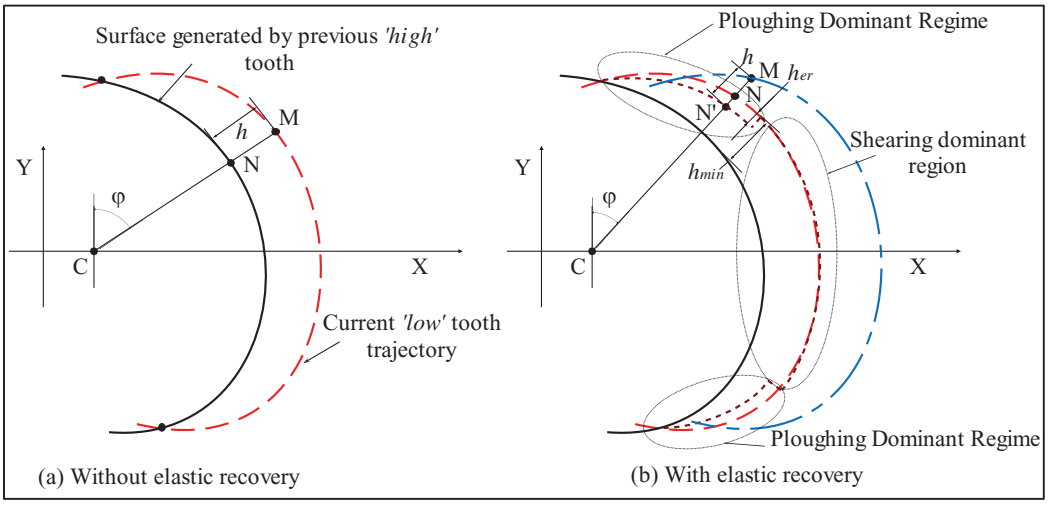

Figure 4. Determination of chip thickness without and with elastic recovery

$$\left.\begin{aligned} x'(k,i) &= x(k,i) - h_{er}\sin(\varphi) \\ y'(k,i) &= y(k,i) - h_{er}\cos(\varphi) \end{aligned}\right\} \tag{9}$$

In the presence of cutter runout, interactions between tooth trajectories must be considered to compute chip thickness realistically. The instantaneous uncut chip thickness for a *'low'* tooth is calculated as radial distance between current tooth trajectory and surface generated by previous *'high'* tooth. But, computing chip thickness for a *'high'* tooth requires determining two distances. Firstly, the radial distance between current trajectory and surface generated by immediately previous *'low'* tooth (from A to B as shown in Figure 5) and secondly, the radial distance between current tooth trajectory and surface generated by previous *'high'* tooth (from C to A and B to D in Figure 5). Here, A and B are entry and exit points of previous *'low'* tooth trajectory, whereas, C and D are entry and exit points of current *'high'* tooth trajectory as shown in Figure 5. It can be seen that the current *'high'* tooth trajectory interacts not only with the preceding *'low'* tooth trajectory but also with the *'high'* tooth trajectory. If such tooth trajectory interactions are not considered, E and F will be determined as entry and exit points instead of C and D which are determined considering interactions of trajectories. For Case-III, the *'low'* tooth is not engaged in the cut and material is not removed by the same however, *'high'* tooth is removing all the material. Therefore, the instantaneous uncut chip thickness removed by *'high'* tooth is computed as the radial distance between the current trajectory of *'high'* tooth and surface generated by previous *'high'* tooth.

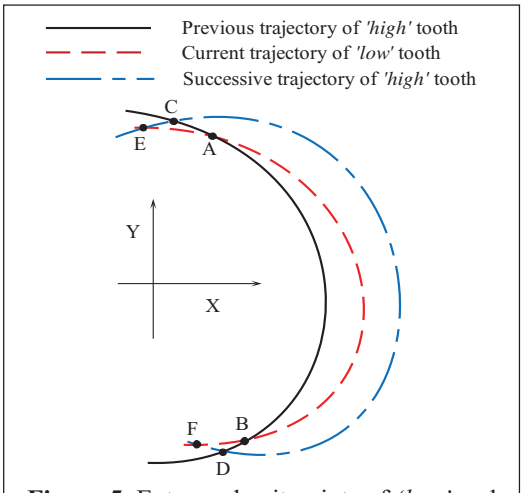

Figure 5. Entry and exit points of *'low'* and *'high'* tooth for case-II

3 Results and Discussion

The model outlined in previous section has been implemented in the form of a computational program to determine process geometry parameters. This section summarizes results obtained from the proposed model and discusses the effect of cutter runout and elastic recovery of work material on process geometry parameters. The engagement angle is determined with and without cutter runout as well as at two different runout values. Similarly, the effect of cutter runout on instantaneous uncut chip thickness is investigated at different feed rate values. The effect of tooth trajectory interactions and elastic recovery of work material has been also assessed on process geometry parameters. The cutter runout offset values of 0.5 and 1µm along with 45° orientation angle is selected for the computational studies. The elastic recovery rate is obtained from scratch test as 10% for Aluminium and minimum chip thickness is taken as 30% of the edge radius (Malekian et al. 2009). Table 1 lists parameters related to geometry of a cutting tool and other cutting conditions used in the study. The results obtained from process geometry model are presented for the bottom most axial disc element in this section. Although results are presented in this paper for a two flute end mill which is quite common in micro-milling, the developed methodology is general and can be extended to any cutter.

Table 1. Tool geometry and cutting conditions

Tool diameter, d	1mm
Edge radius, r_e	2µm
Helix angle, θ_{hx}	30°
Elastic recovery rate of Aluminium, p_e	0.1
Number of teeth, N_t	2
Axial depth of cut, A_{DOF}	50µm
Radial depth of cut, R_{DOF}	1mm (full immersion)
Minimum chip thickness, h_{min}	0.3*r_e
Feed per tooth, fpt	10,8,6,5,4,3,2,1.5, 1,0.75,0.5 m/tooth
Tool runout offset, ρ	0, 0.5, 1.0 µm
Tool runout orientation angle, γ	45°

3.1 Engagement Angle

As discussed in Section 2, engagement angle is computed using coordinates of tool centre point and intersection points obtained using current tooth trajectory and previous tooth surfaces as per the nature of engagement. The computational model determines entry and exit angles initially as it decides lower and upper bounds respectively. Figures 6 and 7 show computational results for entry and exit angle of a *'high'* and *'low'* cutting edge at different values of feed per tooth and cutter runout. It can be seen from Figures 6 and 7 that the effect of cutter runout is negligible on entry and exit angle of a *'high'* tooth. However, it has significant effect on entry and exit angle of a *'low'* tooth. It is evident from Figure 6(b) that the entry of *'low'* tooth is significantly late in the cut at lower feed per tooth values. It can be observed from Figure 7(b) that the *'low'* tooth also exits quite early from the cut at lower feed per tooth values. It can be seen that the methodology does not predict entry and exit angle values for a *'low'* tooth below feed rate of 1µm/tooth at runout offset of 1µm. It implies that a *'low'* tooth is not engaged in the cut when feed per tooth is less than the magnitude of cutter runout. As the cutting edge corresponding to a *'low'* tooth is not engaged with the workpiece, it does not remove work material, leaving it to be removed by a *'high'* tooth in subsequent pass.

Figure 8 shows the effect of cutter runout offset and feed per tooth on engagement angle. It can be seen that the change in engagement angle for a '*high*' tooth is negligible but engagement of '*low*' tooth is significantly altered. The engagement angle of a 'low' tooth is reduced significantly at lower values of feed per tooth. This can be explained from the variation of entry and exit angles discussed earlier. It can be concluded that the cutter runout has prominent effect on engagement angle for a 'low' tooth at smaller values of feed per tooth. It can also be concluded that the '*low*' tooth is not engaged in the cut when feed per tooth is less than the magnitude of cutter runout.

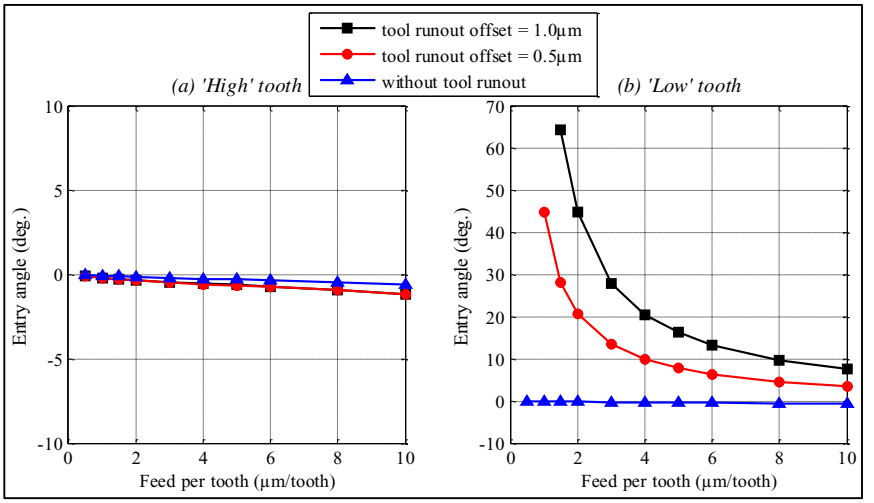

Figure 6. Variation of entry angle with runout offset and feed per tooth

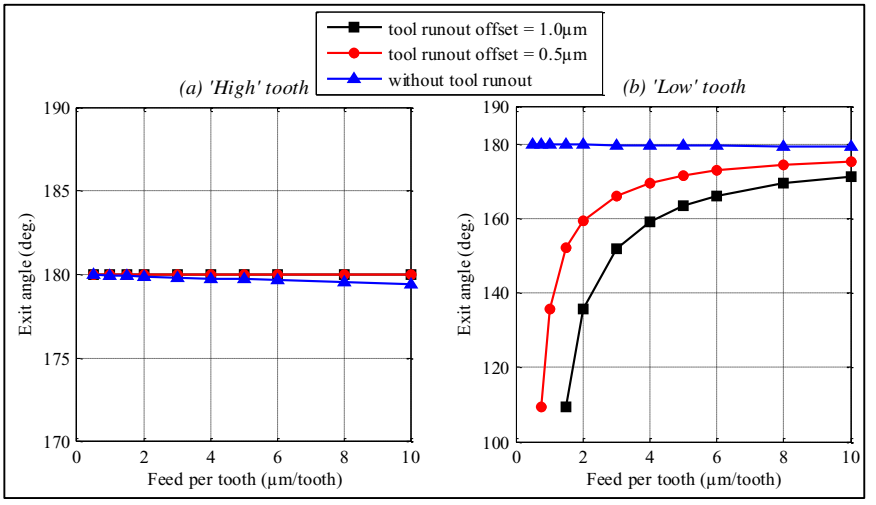

Figure 7. Variation of exit angle with runout offset and feed per tooth

It has been highlighted in Section 2 that the tooth trajectory under consideration can interact with more than one preceding tooth trajectories in the presence of cutter runout. It has been also realized in Section 2 that the trajectory of a '*low*' tooth always interacts with immediately previous tooth trajectory except engagement case-III where there are no interactions. However, a '*high*' tooth trajectory may interact with previous '*low*' tooth trajectory or previous '*high*' tooth trajectory depending on the engagement case. Due to these reasons, engagement angle is computed using two approaches: first, without considering interactions of tooth trajectories and second, considering the interactions. The entry, exit and engagement angle for a '*high*' and '*low*' tooth has been computed using these two approaches and results are shown in Figure 9.

Figure 9(a) shows variation of entry angle of a '*high*' tooth with the feed rate. It can be seen that the approach not incorporating tooth trajectory interactions predicts considerably higher value of entry angle than the approach which considers the same. The difference between entry angle values predicted using both approaches vary significantly at lower feed rates.

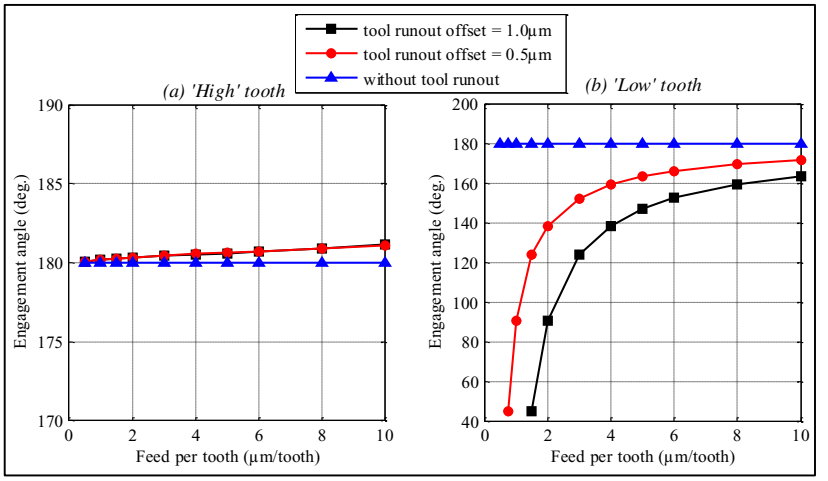

Figure 8. Variation of engagement angle with runout offset and feed per tooth

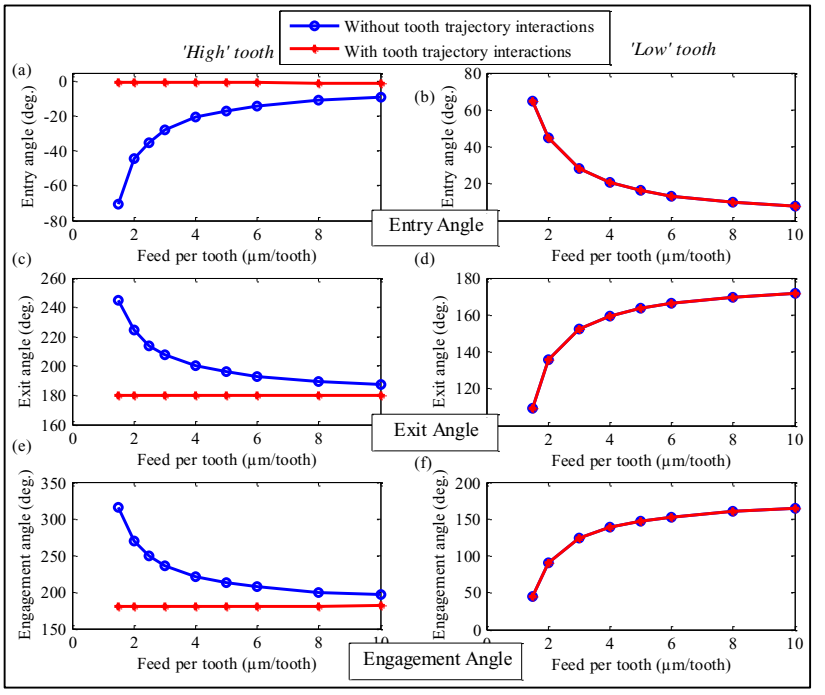

Figure 9. Comparison of entry, exit and engagement angles with and without tooth trajectory interactions

Figure 9(b) shows variation of entry angle for a *'low'* tooth. It can be seen that the value of entry angle predicted using both approaches is identical. As *'low'* tooth always interacts with the immediately preceding tooth trajectory, both approaches predict the same value of exit angle. In the presence of cutter runout, it is expected that a *'high'* tooth engages longer and cuts more whereas, a *'low'* tooth engages shorter and cuts less. But, the same is not observed when interactions of tooth trajectories are considered. The *'low'* tooth cuts as expected but the behaviour of a *'high'* tooth is significantly different. Due to interactions of trajectories, *'high'* tooth does not engage early and exits in the same manner as without cutter runout. Thus entry and exit angle for a *'high'* tooth shows significant differences while computing

results with both approaches (Figure 9(a) and (c)). However, entry and exit angles of a *'low'* tooth are the same (Figure 9(b) and (d)). The behaviour of engagement angle for a *'high'* and *'low'* tooth with and without tooth trajectory interactions is also depicted in Figure 9(e) and (f) respectively. The same can be correlated with the variation of entry and exit angles as engagement angle is computed from both.

Another important aspect of micro-milling operation is the elastic recovery of work material. Due to elastic recovery of work material, entry and exit points can change in a ploughing dominant region leading to change of engagement angle. Referring to Figure 3(b), entry and exit points of current '*high*' tooth trajectory changes to P'_2 and Q'_2 instead of P_2 and Q_2. It has been observed that the difference in coordinates of tooth entry and exit points before and after elastic recovery is very small and can be neglected. This is primarily due to very small value of chip thickness and elastic recovery height at these points.

3.2 Instantaneous Uncut Chip Thickness

It has been observed in the previous section that the engagement behaviour of a *'low'* tooth is significantly different from a *'high'* tooth at lower values of feed rate. It implies that the chip load acting on both teeth will be significantly different. Figure 10 shows variation of instantaneous uncut chip thickness for *'high'* and *'low'* teeth at different values of feed per tooth and in the presence and absence of cutter runout for one revolution of the cutter. Although engagement angle for a *'high'* tooth does not increase in the presence of cutter runout, the chip load is increased significantly. This shows that the *'high'* tooth is removing larger amount of material in comparison to a *'low'* tooth. This can also be seen from results in Figure 10(a) and (b). The cases presented in Figure 10(a) and (b) are similar to engagement Case-II. For lower values of feed per tooth (e.g. 1 and 0.5µm/tooth), the engagement nature of cutting teeth is similar to engagement Case-III. It can be seen that a *'low'* tooth is not engaged in the cut and *'high'* tooth removes entire material during revolution of a cutter which increases chip load significantly (Figure 10(c) and (d)).

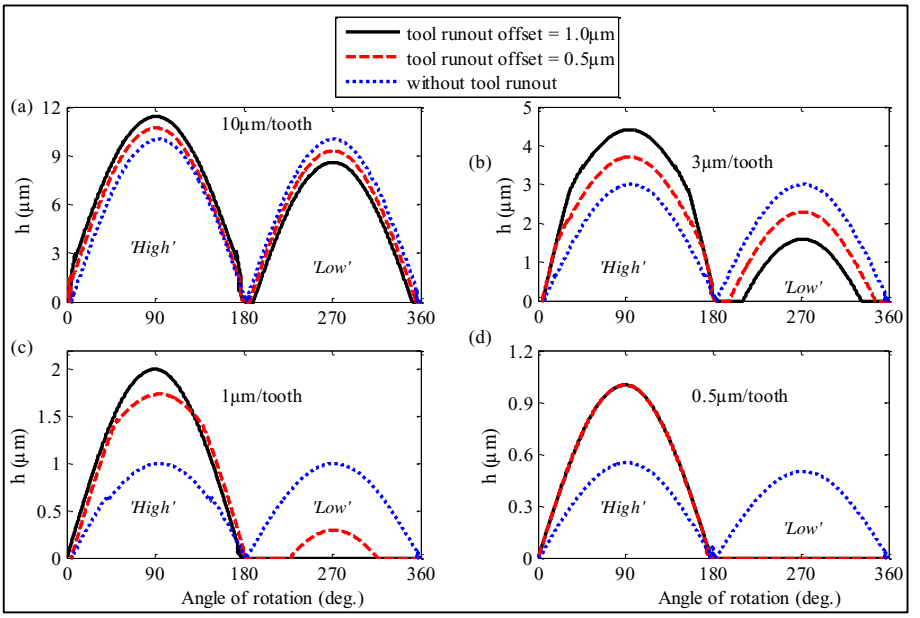

Figure 10. Instantaneous uncut chip thickness variation with feed per tooth and cutter runout

The results of instantaneous uncut chip thickness clearly indicate that cutter runout has marked effect at lower values of feed rate. The value of maximum uncut chip thickness in slot milling is same as feed per tooth in the absence of cutter runout. However, the same does not happen when cutter runout is

present and instantaneous chip thickness for *'high'* tooth is quite larger. The percentage variation of maximum uncut chip thickness between *'low'* and *'high'* tooth is shown in Table 2. The results of Table 2 are computed at 1µm cutter runout using model proposed in this paper. It can be seen that the maximum chip thickness removed by a *'low'* tooth is about 14% lower at 10µm feed per tooth whereas it is increased by the same percentage for a *'high'* tooth. At lower values of feed rate, the percentage change in maximum chip thickness between two teeth is pronounced. When feed per tooth is of the same magnitude or less than the cutter runout, *'low'* tooth does not remove any material. For such cases, the maximum uncut chip thickness removed by *'high'* tooth is twice the feed rate value.

Table 2. Maximum Uncut chip thickness, h_{max} with Percentage Change

fpt (µm/tooth)		10	8	4	2	1	0.5
h_{max}(µm) at ρ =1µm	*'low'* tooth	8.59	6.59	2.59	0.54	0.0	0.0
	'high' tooth	11.41	9.41	5.41	3.46	2.0	1.0
Percentage change (%)		24.72	29.97	52.12	84.39	100.0	100.0

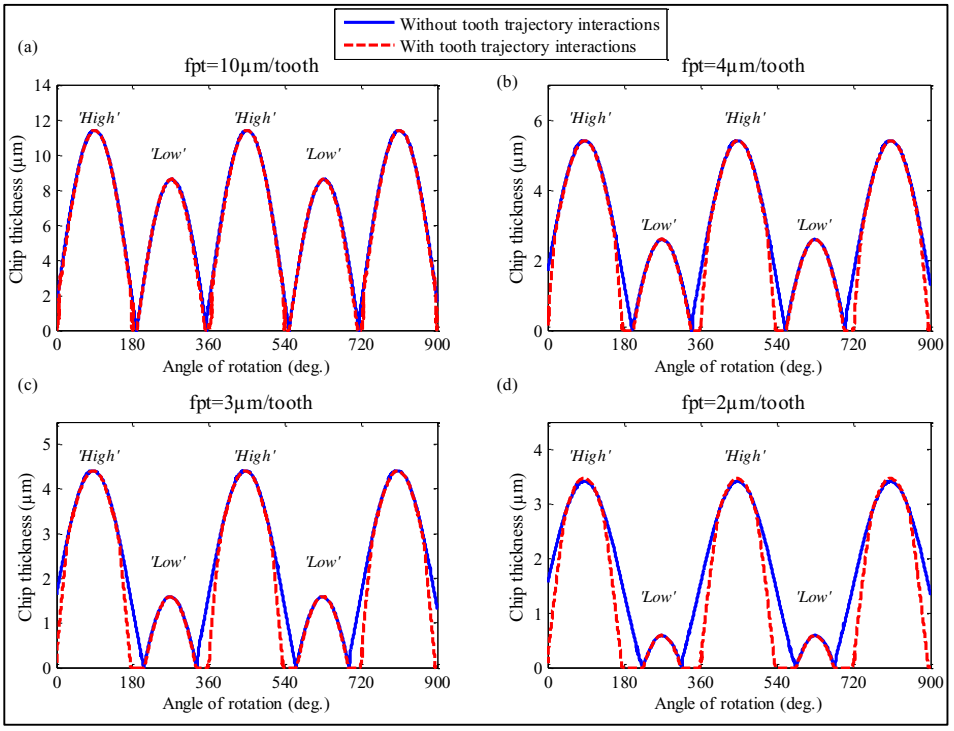

Figure 11. Comparison of chip thickness with and without tooth trajectory interactions

It has been discussed earlier that the inclusion of tooth trajectory interactions change predicted value of engagement angle significantly. In order to examine the effect of tooth trajectory interactions, chip thickness has been computed using both approaches: with and without tooth trajectory interactions and the results are shown in Figure 11. It can be seen that the chip thickness values predicted using both approaches are identical at higher feed rate values (Figure 11(a)). This can be attributed to interaction of two successive tooth trajectory for each tooth. With reduction of feed rate, the difference between predictions of both approaches commences and it increases further. It can be seen that the uncut chip thickness at the start and end of *'high'* tooth engagement is not predicted well but the same is not true for *'low'* tooth (Figure 11(b)). The difference of prediction for *'high'* tooth is primarily due to inclusion of tooth trajectories interactions in the process geometry model. The difference of prediction is quite higher at lower feed rates (Figure 11(c) and (d)). The approach ignoring interactions of tooth trajectories

predicts higher values of engagement angle and instantaneous uncut chip thickness for a *'high'* tooth. From the comparison of results obtained using both approaches, it can be inferred that the inclusion of tooth trajectory interactions should be included in the model as it leads to significant difference in prediction of process geometry parameters.

Although the effect of elastic recovery on engagement angle is not significant, it has substantial effect on chip thickness values at small feed rates. Figure 12 shows the effect of elastic recovery on instantaneous uncut chip thickness. The minimum chip thickness value has been determined as 0.6µm for given work material in the present study. At feed rate value of 0.2µm/tooth, '*high*' tooth is engaged in the cut whereas '*low*' tooth is not removing the material due to cutter runout (Figure 12(b)). A '*low*' tooth is not engaged in the cut as maximum chip thickness is less than the minimum limiting value and chip formation does not occur. For each successive tooth pass, the chip thickness increases by an amount of elastic recovery height (h_{er}) and the same continues until the minimum value of chip thickness is reached. When there is no elastic recovery, the chip thickness is identical for each tooth pass. This can be observed for a '*low*' tooth at feed per tooth value of 2µm/tooth (Figure 12(a)). The effect of elastic recovery for a '*high*' tooth is insignificant as the chip thickness is greater than the minimum limiting value. From the results outlined in this section, it can be seen that elastic recovery of work material has significant influence on the instantaneous uncut chip thickness at small feed per tooth values.

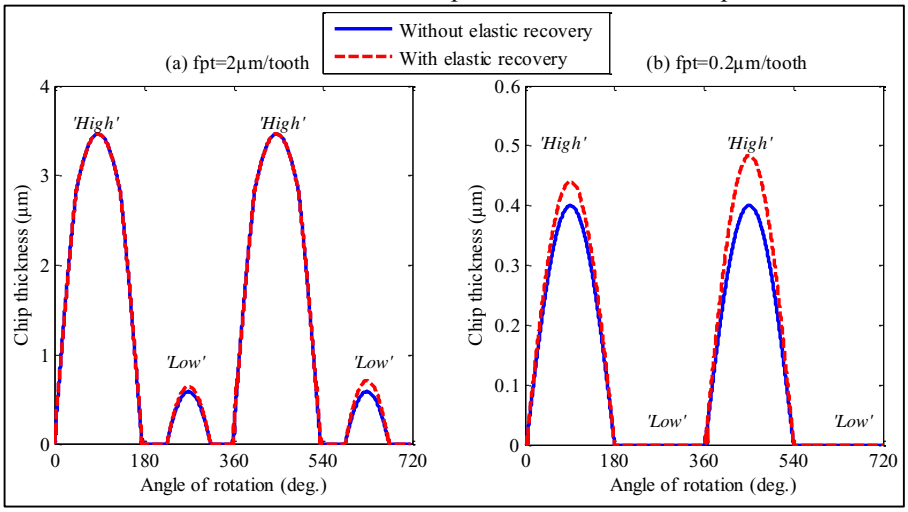

Figure 12. Effect of elastic recovery on instantaneous uncut chip thickness

3.3 Experimental Results and Model Validation

As process geometry parameters are closely linked with magnitude and profile of cutting forces, experimentally measured forces can be used to assess the effectiveness of the proposed model. For this purpose, a set of micro-milling experiments have been conducted using solid carbide end mill of 1mm diameter with 30° helix angle and two flutes. A set of full immersion machining experiments are performed on Aluminium 6351-T6 at 0.1mm axial depth of cut and different feed rate values. The edge radius of the micro-end mill is approximately 2µm and the elastic recovery rate of the workpiece material is known to be 10% from scratch test. The minimum chip thickness of Aluminium is approximately 30% of the edge radius (Malekian et al., 2009). The measured value of cutter runout is 0.75µm and orientation angle is considered to be 45°. The experiments are conducted on a CNC vertical milling machine and cutting forces are measured using piezo-electric dynamometer. The measured forces in F_x and F_y are recorded as a function of time using data acquisition software. The instantaneous resultant force has been obtained from measured forces F_x and F_y and the same is used to evaluate the

effectiveness of the proposed model. While conducting machining experiments, two sets of force signals are collected: without tool-workpiece contact due to spindle rotation (air cutting) and with tool-workpiece engagement. The measured cutting forces are obtained by synchronizing the two signals and subtracting the force signal during air cutting from tool-workpiece engagement force signal. The measured force signal is recorded as a function of time and the same is transformed to angular rotation of the cutter to extract engagement angle.

Figure 13 shows measured instantaneous resultant cutting force for different values of feed per tooth. It can be seen that a *'high'* tooth is subjected to significantly larger cutting forces than the *'low'* tooth as later engages lately in the cut and exit early removing lesser material. It can be seen from Figure 13(a) to (d) that the magnitude and profile of resultant force shows similar trend with instantaneous uncut chip thickness at various feed per tooth. As feed per tooth reduces, the *'low'* tooth contributes lesser in removing the material and thus the resultant forces also decrease substantially (Figure 13(b) and (c)). With further reduction of feed per tooth (Figure 13(d)), the *'low'* tooth does not engage in the cut at all and resultant forces approach to zero. Such behaviour of resultant forces at different feed per tooth can also be substantiated using instantaneous uncut chip thickness highlighted in earlier section.

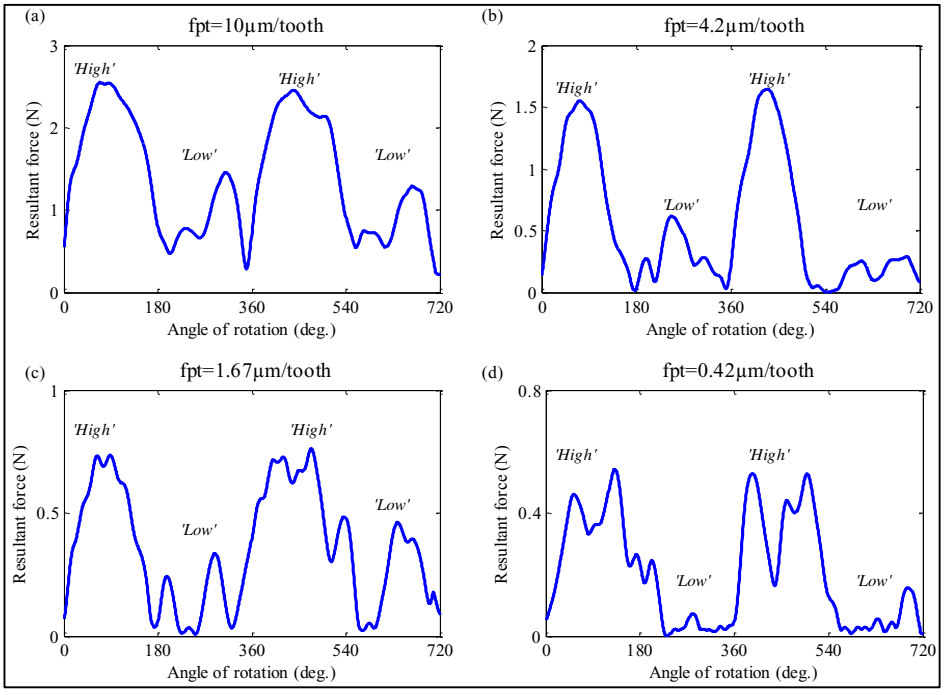

Figure 13. Measured instantaneous resultant force

Table 3 summarizes engagement angle of a *'high'* tooth predicted using both approaches and comparison of the same with its measured counterparts obtained from resultant cutting forces. An important point to note here is the effect of sweep angle in axial direction due to helix angle has been added in the engagement angle. The sweep angle in axial direction is due to helix angle of the cutter and can be calculated from the last term of Equation (2) by replacing k and dz by number of axial disk elements and axial depth of cut, respectively. As discussed earlier, both approaches predict identical value of engagement angle for a *'low'* tooth. But the predicted value of engagement angle for a *'high'* tooth is significantly different with both approaches. This can be attributed to inclusion of tooth trajectory interactions in process geometry model. It can be seen that the approach considering tooth trajectory interactions predict engagement angle for a *'high'* tooth better. The approach ignoring tooth trajectory interactions assumes that the given trajectory interacts with its immediately previous tooth

trajectory only. As trajectory interactions are not considered in the model, larger value of engagement angle and instantaneous uncut chip thickness are predicted for a *'high'* tooth. Based on the results outlined in this section, it can be concluded that the process geometry parameters can be predicted accurately using the approach presented in this study which considers tooth trajectory interactions in the presence of tool runout for micro-milling operation.

Table 3. Comparison of predicted and measured engagement angle of *'high'* tooth

fpt (μm/tooth)	Without interactions	With interactions	Measured value
10	198.5°	187.7°	188°
4.2	215.9°	186.9°	186°
1.67	260.4°	186.8°	187°
0.42	--	186.6°	186°

4 Conclusions

This paper presented a comprehensive process geometry model for micro-milling operation considering true trajectory of cutting teeth, cutter runout and elastic recovery of work material. The paper analysed the engagement region and considered interactions between cutting tooth trajectories to determine engagement angle and instantaneous uncut chip thickness. The proposed model is implemented in the form of a computational program to study and analyse the variation of engagement angle and instantaneous uncut chip thickness at different values of feed rate. The paper also studied the effect of cutter runout offset and elastic recovery of workpiece material on these parameters. The effectiveness of the proposed process geometry model is validated by conducting micro-milling experiments at various feed per tooth values. The following conclusions have been drawn from the present work.

- It has been observed that the engagement angle of a *'low'* tooth reduces substantially in the presence of cutter runout while it remains the same for *'high'* tooth when tooth trajectory interactions are considered. The reduction of engagement angle is significant at lower values of feed per tooth. It has been observed in the previous studies (Afazov et al. 2010) that the engagement angle of *'high'* tooth increases considerably in the presence of cutter runout but the same does not happen when trajectory interactions are considered. The same has been substantiated further by conducting machining experiments at different cutting conditions.
- The instantaneous uncut chip thickness of a *'high'* tooth is influenced significantly in the presence of cutter runout. The *'high'* tooth experiences significantly higher chip load than a *'low'* tooth as the later enters the cut lately and exits early. The difference in chip load experienced by each tooth is quite higher at lower values of feed rate.
- In order to predict process geometry parameters accurately in the presence of cutter runout, it is necessary to consider interaction of current tooth trajectory with more than one preceding tooth trajectories. If the same is not considered, the engagement angle and instantaneous uncut chip thickness of *'high'* tooth will be substantially different.
- The elastic recovery of work material has significant effect on process geometry parameters when chip thickness is less than the limiting minimum value.

The model outlined in this paper presents a methodology to predict process geometry parameters accurately during micro-milling. The model can be linked directly with the cutting forces model and will be extended further in future to predict forces accurately during micro-milling.

Acknowledgements

The authors thank Dr. J RamKumar, Mechanical Engineering Department, IIT Kanpur and Mr. Kinde Anley Fante research scholar at IIT Delhi for useful support during the course of present work.

References

Afazov SM, Ratchev SM and Segal J. Modelling and simulation of micro-milling cutting forces. *Journal of Materials Processing Technology* 2010; 210(15): 2154–2162.

Altintas Y. Manufacturing Automation: *Metal Cutting Mechanics, Machine Tool Vibrations and CNC Design.* Cambridge: Cambridge University Press, 2000.

Bao WY and Tansel IN. Modeling micro-end-milling operations. Part I : analytical cutting force model. *International Journal of Machine Tools and Manufacture* 2000a; 40: 2155–2173.

Bao WY, Tansel IN. Modeling micro-end-milling operations. Part II : tool run-out. *International Journal of Machine Tools and Manufacture* 2000b; 40: 2175–2192.

Chae J, Park SS and Freiheit T. Investigation of micro-cutting operations. *International Journal of Machine Tools and Manufacture* 2006; 46(3-4): 313–332.

Cheng K and Huo D. Micro-Cutting Fundamentals and Applications. UK: John Wiley & Sons Ltd, 2013.

Desai K, Agarwal PK and Rao PVM. Process geometry modelling with cutter runout for milling of curved surfaces. *International Journal of Machine Tools and Manufacture* 2009; 49(12-13): 1015–1028.

De Oliveira FB, Rodrigues AR, Coelho RT and De Souza AF, Size effect and minimum chip thickness in micromilling. *International Journal of Machine Tools and Manufacture 2015;* 89; 39–54.

Jing X, Li H, Wang J and Tian Y. Modelling the Cutting Forces in Micro-end-milling Using a Hybrid Approach. *The International Journal of Advanced Manufacturing Technology* 2014; 73(9-12): 1647–1656.

Jun MBG, Goo C, Malekian M and Park S. A New Mechanistic Approach for Micro End Milling Force Modeling. *Journal of Manufacturing Science and Engineering* 2012; 134(1): 011006-9.

Jun MBG, Liu X, DeVor RE and Kapoor SG. Investigation of the Dynamics of Microend Milling—Part I: Model Development. *Journal of Manufacturing Science and Engineering* 2006; 128(4): 893-900.

Kang YH and Zheng CM. Mathematical Modelling of Chip Thickness in Micro-end- Milling: A Fourier Modelling. *Applied Mathematical Modelling* 2013; 37(6): 4208–4223.

Kim CJ, Mayor JR and Ni J. A Static Model of Chip Formation in Microscale Milling. *Journal of Manufacturing Science and Engineering* 2004; 126(4): 710-718.

Liu X, DeVor RE, Kapoor SG and Ehmann KF. The Mechanics of Machining at the Microscale: Assessment of the Current State of the Science. *Journal of Manufacturing Science and Engineering* 2004; 126(4): 666-678.

Malekian M, Mostofa MG, Park SS and Jun MBG. Modeling of minimum uncut chip thickness in micro machining of aluminum. *Journal of Materials Processing Technology* 2012; 212(3): 553–559.

Malekian M, Park SS and Jun MBG. Modeling of dynamic micro-milling cutting forces. *International Journal of Machine Tools and Manufacture* 2009; 49(7-8): 586–598.

Martelloti ME. An analysis of the milling process. *Transactions of the ASME* 1941; 63: 677–700.

Martellotti ME. An analysis of the milling process, Part II-Down milling. *Transactions of the ASME* 1945; 67: 233–251.

Park SS and Malekian M. Mechanistic modeling and accurate measurement of micro end milling forces. *CIRP Annals - Manufacturing Technology* 2009; 58(1): 49–52.

Srinivasa, YV and Shunmugam MS. Mechanistic Model for Prediction of Cutting Forces in Micro End-milling and Experimental Comparison. *International Journal of Machine Tools and Manufacture* 2013; 67: 18–27.

Tlusty J and Macneil P. Dynamics of cutting forces in end milling. *CIRP Annals* 1975; 24: 21–25.

Uriarte L, Azcárate S, Herrero A, Lopez de Lacalle LN and Lamikiz A. Mechanistic modelling of the micro end milling operation. *Proceedings of the IMechE, Part B: Journal of Engineering Manufacture* 2008; 222(1): 23–33.

Vogler MP, Kapoor SG and DeVor RE. On the Modeling and Analysis of Machining Performance in Micro-Endmilling, Part II: Cutting Force Prediction. *Journal of Manufacturing Science and Engineering* 2004; 126(4): 695-705.

Weule H, Hüntrup V and Tritschler H. Micro-cutting of steel to meet new requirements in miniaturization. *CIRP Annals - Manufacturing Technology* 2001; 50(1): 61– 64.

Wu T, Cheng K and Rakowski R. Investigation on tooling geometrical effects of micro tools and the associated micro milling performance. *Proceedings of the IMechE, Part B: Journal of Engineering Manufacture* 2012; 226(9): 1442–1453.

Nomenclature

r	Tool radius (mm)	d	Tool diameter (mm)
N_t	Number of teeth	θ_{hx}	Helix angle of cutter (°)
φ_p	Pitch angle of cutter (°)	θ	Angle of rotation (°)
φ	Instantaneous angular position (°) of i^{th} cutting edge		
i	Index for cutting edge	k	Index for axial disc element
fpt	Feed per tooth (mm/tooth)	ρ	Runout offset (mm)
γ	Runout orientation angle (°)	dz	Axial disc element Thickness (mm)
θ_{entry}	Entry angle (°)	θ_{exit}	Exit angle (°)
θ_{eng}	Engagement angle (°)	h	Instantaneous chip thickness (mm)
h_{er}	Elastic recovery height (mm)	h_{min}	Minimum chip thickness (mm)
p_e	Elastic recovery rate (%)	r_e	Edge radius (mm)
F_x, F_y and F_r	Dynamometer measured force in X and Y direction and Resultant force (N)		